Mechanical, Thermal Stability, and Flame Retarding Properties of Phosphorus-Modified PET Blended with DOPO-POSS

Anying Zhang, Wenhui Wang, Zhenfeng Dong, Jianfei Wei, Lifei Wei, Weiwen Gu, Guo Zheng,* and Rui Wang*

ACCESS | Metrics & More | Article Recommendations

ABSTRACT: In this study, an antidroplet flame retardant system based on FRPET (phosphorus-containing copolyester) is constructed with DOPO-POSS (polyhedral oligomeric silsesquioxane containing DOPO) as an additive flame retardant. It is demonstrated that DOPO-POSS has good dispersibility at a lower amount. When the amount of DOPO-POSS is 9 wt %, the residual char of DOPO-POSS/FRPET at 700 °C increases to 23.56 from 18.16% of FRPET, and the maximum thermal weight loss rate also reduces. What is more is that the limiting oxygen index increases to 33 from 26% of FRPET. The flame burning time is shortened to 4.95 from 20.8 s, the phenomenon of self-extinguishing of the fire occurs, and the vertical combustion level is increased from V-2 to V-0. Compared with FRPET, the peak of the heat release rate decreases by 66.0%, the total heat release decreases by 32.4%, the flame retardancy index (FRI) reaches an excellent value, and the condensed-phase products significantly improve. The Fourier transform infrared spectroscopy (FTIR), scanning electron microscopy−energy dispersive X-ray spectrometry (SEM−EDX), thermogravimetric−FTIR (TG−FTIR), and pyrolysis−gas chromatograph/mass spectrometry (Py−GC/MS) results indicate that DOPO-POSS contributes to the formation of char layers and decomposes to generate free radicals with a quenching effect. In a word, DOPO-POSS is an effective radical trapper and charring agent for PET and exerts a flame retardancy effect in gaseous and condensed phases simultaneously.
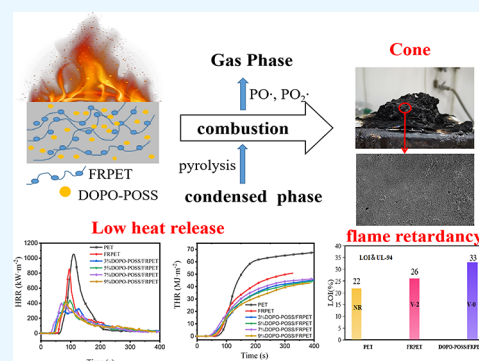
1. INTRODUCTION

As a saturated aromatic thermoplastic polyester, poly(ethylene terephthalate) (PET) is widely used in the automotive industry, packaging and home textiles due to its excellent comprehensive properties, including high strength, high modulus, chemical resistance, spinnability and low cost.[1,2] However, PET is a flammable material and the limiting oxygen index (LOI) of PET is only 22%. In addition, due to the linear structure of PET, droplets are easily generated during the combustion process, which accelerate the spread of flames.[3,4] There are safety hazards due to the inflammability and widespread use of PET, especially mainly in traffic interior decoration, cable protection, and other fields. Therefore, it is important to prepare PET with flame retardancy and droplet resistance simultaneously, and it has been one of the hotspots in the flame retardant field.[5,6]

At present, the common modification methods for preparing flame-retardant PET mainly include blending and copolymerization. Blending modification usually refers to introducing flame retardants into PET through melt extrusion, so its advantages include simple process, flexible adjustment and low production cost. N.Didane's[7] group used a zinc phosphinate fire retardant (Exolit OP950) and three polyhedral oligomeric

silsesquioxanes (POSS) and then blended them with PET to obtain a new type of flame retardant polyester. Regardless of the POSS type, intumescence occurs during combustion, but the insulation properties of the chars produced are different. Compared with blends, the flame-retardant PET prepared by copolymerization has better durability and uniformity. However, the requirements for flame retardants are relatively high and the preparation process is also more complicated.[8]

2-Carboxyethyl hypophosphorous acid (CEPPA) is a kind of organophosphorus flame retardant, which is widely used in the copolymerization flame retardant modification of PET. The addition of CEPPA to PET can effectively improve the limiting oxygen index and thermal stability of PET. During the combustion process, PO$^{\bullet}$ and HPO$^{\bullet}$ radicals released by CEPPA are generated to capture H$^{\bullet}$ and OH$^{\bullet}$ free radicals to inhibit chain reactions in the gas phase. In addition, it also can

decompose to produce phosphoric acid and metaphosphoric acid, which cover the surface of the polymer to protect the inner polymer from further oxidative degradation in the condensed phase.[9,10]

Silicon-based compounds are also effective additives to improve the flame retardancy of PET, such as polyhedral oligomeric silsesquioxane (POSS), which is a cage compound formed by Si−O bonds.[11,12] The cage structure not only gives it good stability but also forms a continuous protective solid layer after burning, covering combustible materials, which prevents the combination of combustible gas and air, preventing heat transfer and then slowing the spread of flames. The structure of DOPO-POSS is shown in Figure 1.[13,14] The R
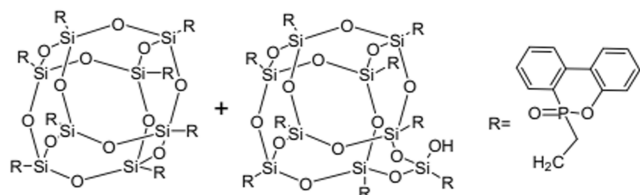

Figure 1. Structure of DOPO-POSS.

group of DOPO-POSS is the phosphine compound 9,10-dihydro-9-oxo-10-oxide (DOPO). The phosphorus-containing group O=P−O of DOPO located in the pendant group can provide higher hydrolytic stability and inhibit the occurrence of the droplet phenomenon during combustion.[15,16] Based on the previous experience, a phosphor−silicone composite flame retardant system is constructed and then applied in PET to obtain a flame-retardant and antidripping flame-retardant polyester.[17,18]

In this paper, 6500 ppm-phosphorus content FRPET was prepared by polymerization, and then, DOPO-POSS was blended with FRPET to obtain FRPET/DOPO-POSS. The dispersibility, thermal stability, flame retardancy, and mechanical properties of the flame-retardant polyester were analyzed. In addition, the flame retardancy mechanism of the flame retardant was also explored.

2. EXPERIMENTAL SECTION

2.1. Materials. Poly(ethylene terephthalate) (PET) was purchased from Sichuan EM Technology Co.,Ltd. FRPET is a flame-retardant PET with CEPPA as the flame retardant provided by Dongoingying Merida New Material Technology Co.,Ltd. DOPO-containing polyhedral oligomeric silsesquioxane (DOPO-POSS) was supplied by the Beijing Institute of Technology (Figure 1).

2.2. Preparation of Flame-Retardant PET Composites. First, PET (or FRPET) was put into a pulverizer and liquid nitrogen was poured into the pulverizer for quenching and then pulverized. Then, the PET (or FRPET) and DOPO-POSS were dried in a vacuum oven (vacuum drying box, DZF-6050, Shanghai Yiheng Technology Co, Ltd.) at 130 and 80 °C for 12 h before use. The FRPET was blended with the flame retardant using a twin-screw extruder (PolyOS, HAAKE, Germany), the rotation speed is 40 rpm, and the temperature of each zone of the twin screw is 260, 250, 250, 250, 250, and 260 °C. The extrudate was quenched in a water bath, and the composite was then cut into pellets and finally dried in a vacuum oven at 130 °C for 12 h. The compositions of the formulations used in this study are described in Table 1.

Table 1. Formulations of DOPO-POSS/FRPET

sample	FRPET (wt %)	DOPO-POSS (wt %)
PET		
FRPET	100	0
3%DOPO-POSS/FRPET	97	3
5%DOPO-POSS/FRPET	95	5
7%DOPO-POSS/FRPET	93	7
9%DOPO-POSS/FRPET	91	9

2.3. Characterizations and Testing. A scanning electron microscopy (SEM) experiment was carried out for the morphology features using a JEOL JSM-7500 scanning electron microscope of Japan Electronics Co., Ltd.

2.3.1. Differential Scanning Calorimetry (DSC). First, it is heated on a melting hot table (300 °C) and then quenched to eliminate the thermal history, and DSC (merican TA company Q2000) was used to investigate the thermal transition behavior of the composites. The samples weigh about 5−8 mg, and the temperature range is 30−300 °C. The samples are heated to 300 from 30 °C at a ramp rate of 10 °C·min^{-1} before it decreased from 300 to 30 °C at 10 °C·min^{-1}.

2.3.2. Thermogravimetric Analysis (TGA). Thermogravimetric analysis was performed using a Netzsch TG 209 F1 (Netzsch, Germany) instrument. About 5 ~10 mg of the sample was put in an alumina crucible and heated from ambient temperature to 700 °C. The heating rate was set as 10 °C·min^{-1} (nitrogen atmosphere, flow rate of 20 mL·min^{-1}).

2.3.3. Fourier Transform Infrared (FTIR). FTIR spectra were collected on a Nicolet Nexus 670 FTIR spectrometer (Thermo Fisher Scientific, Waltham, MA) using the ATR method, at ambient temperature. The spectra were collected in the optical range of 400−4000 cm^{-1} with a scanning number of 64.

2.3.4. Cone Calorimetery Test (CCT). The cone calorimetery (Stanton Redcroft, U.K.) tests were performed according to the ISO 5660 standard procedures. Each specimen of dimensions 100 mm × 100 mm × 3 mm was wrapped in an aluminum foil and exposed horizontally to an external heat flux of 50 kW·m^{-2} with the use of the "frame and grid".

2.3.5. Limiting Oxygen Index (LOI) Test. The LOI value was measured using a Dynisco LOI instrument (Dynisco, American) according to GB/T 2406-80 (sample dimension: 80 mm × 6.5 mm × 3.0 mm). The LOI measurement for each specimen was repeated five times.

2.3.6. Vertical Burning Test. The UL-94 combustion level was characterized using a CZF-3 horizontal and vertical burner instrument according to GB/T5455-1997 (sample dimension: 130 mm × 13.0 mm × 3.0 mm).

2.3.7. Physical and Mechanical Properties. The standard sample for the tensile test was prepared using a MiniJetII micro injection molding machine, and the mechanical strength test of the standard sample was performed using a INSTRON 5966 electronic material testing machine, and the tensile rate was 10 mm·min^{-1}, and the tensile load was 1 kN. Each sample was tested five times, and the results were averaged.

2.3.8. Thermogravimetric−Fourier Transform Infrared (TG−FTIR). The infrared spectrum of the sample pyrolysis gas was measured using the combination of a METTLER TOLEDO thermogravimeter and Nicolet Is50 Fourier infrared spectrometer.

2.3.9. Pyrolysis−Gas Chromatography−Mass Spectrometry (Py−GC−MS). It was performed using a pyrolysis instrument (EGA/PY-3030, Thermo Fisher, Waltham, MA)

equipped with a GCMS-QP2010 Ultra system and carrier in a helium atmosphere. The pyrolysis temperature was 700 °C, the holding time was 300 s, and the heating rate was 200 °C·s⁻¹.

3. RESULTS AND DISCUSSION

3.1. SEM Analysis. SEM images of the fracture surfaces of the FRPET and DOPO-POSS/FRPET composites are shown in Figure 2. It can be seen that the surface of FRPET is flat and
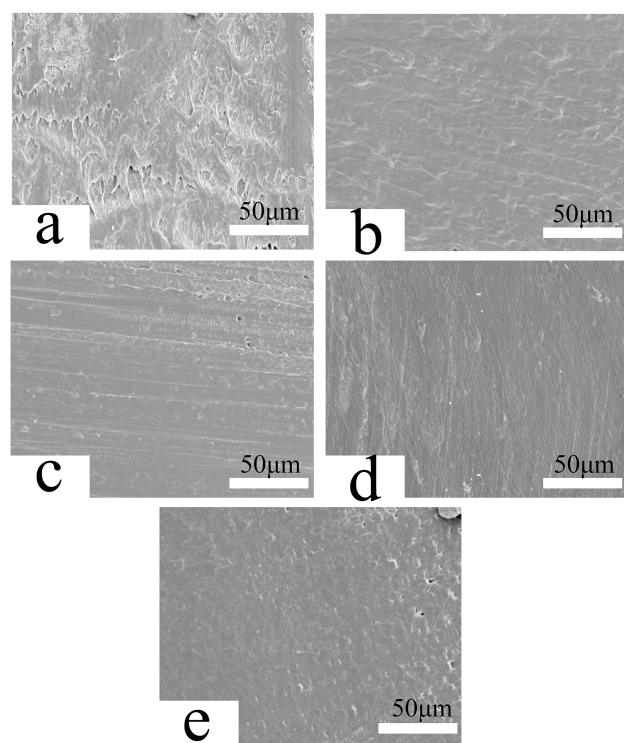
Figure 2. SEM micrographs of fractured surface composites: (a) FRPET, (b) 3%DOPO-POSS/FRPET, (c) 5%DOPO-POSS/FRPET, (d) 7%DOPO-POSS/FRPET, and (e) 9%DOPO-POSS/FRPET.

smooth, and no obvious granular objects are observed.[19] Because the melting point of DOPO-POSS is 234 °C, which is lower than the processing temperature (240−260 °C), DOPO-POSS can have a good dispersibility in FRPET. Moreover, as shown in Figure 2b−e, with increasing amount of DOPO-POSS, the distribution of DOPO-POSS is uniform and there is no obvious agglomeration. As a result, it can be speculated that the DOPO-POSS has good compatibility with the matrix.

3.2. DSC Analysis. Figure 3a,b shows the heating and cooling process curves of PET and composite flame-retardant polyester, and the relevant data of the DSC test are shown in Table 2. As we can see from the chart, the glass transition

Table 2. DSC Data of the PET and PET Composites

samples	T_g (°C)	T_{cc} (°C)	T_m (°C)	T_{mc} (°C)	ΔT_{mc} (°C)
PET	80.2	126.3	254.0	220.7	33.3
FRPET	75.8	137.4	254.5	218.9	35.6
3% DOPO-POSS/ FRPET	76.3	133.8	253.4	213.4	40.0
5% DOPO-POSS/ FRPET	76.2	136.4	253.3	214.5	39.0
7% DOPO-POSS/ FRPET	76.0	134.9	253.7	213.3	40.4
9% DOPO-POSS/ FRPET	76.0	135.3	253.3	214.4	38.9

temperature (T_g) of PET is 80.2 °C, the cold crystallization temperature (T_{cc}) is 126.3 °C, and the thermal crystallization temperature (T_{mc}) is 220.7 °C. Compared with PET, the T_g of FRPET decreased to 75.8 °C because the phosphorus-containing flame retardant was introduced into the PET molecular chain through copolymerization, which improved the mobility of the FRPET molecular chain. The change of regularity of the molecular chain also can be proved by the increase of T_{cc} and the decrease of T_{mc}. Compared with FRPET, with increasing amount of DOPO-POSS, the T_g of the DOPO-POSS/FRPET composite flame-retardant polyester is almost unchanged, indicating that the addition of DOPO-POSS in the blending mode has little effect on the movement of the molecular chain. The degree of subcooling (ΔT_{mc}) is the difference between the melting point (T_m) and T_{mc}, which is used to characterize the difficulty of crystallization.[20,21] When the ΔT_{mc} is small, it is easy to crystallize and the crystallization speed is fast; on the contrary, when the ΔT_{mc} is larger, the crystallization speed is slower and the crystallization is more difficult. It can be seen from Table 2 that the ΔT_{mc} of DOPO-POSS/FRPET composites increased to 40.4 °C compared with that of FRPET, indicating that the crystallization of FRPET is more difficult with the addition of DOPO-POSS. It can explain that the cage steric hindrance of DOPO-POSS decreased the FRPET crystallization performance.

3.3. TG Analysis. TG and DTG curves of PET, FRPET, and DOPO-POSS/FRPET composites are presented in Figure 4a,b. The relevant thermal decomposition data, including $T_{5\%}$, defined as the temperature at 5% weight loss, T_{max}, defined as
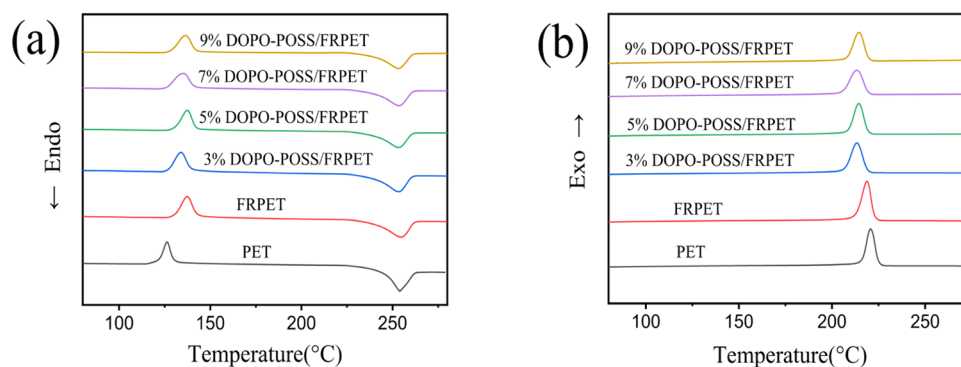
Figure 3. DSC curves of flame-retardant PET composites. (a) Heating curve and (b) cooling curve.

the temperature at maximum weight loss rate, and the char residues at 700 °C, are given in Table 3.

Table 3. TG and DTG Data of PET and PET Composites in N$_2$ at a Heating Rate of 10 °C min^{-1}

samples	$T_{5\%}$ (°C)	T_{max} (°C)	R_{max} (% min^{-1})	C_w (%)
PET	401.51	439.71	21.06	16.97
FRPET	400.27	445.36	19.20	18.16
3%DOPO-POSS/FRPET	402.20	443.24	18.41	19.82
5%DOPO-POSS/FRPET	401.30	439.22	18.35	20.68
7%DOPO-POSS/FRPET	402.03	437.36	18.92	23.70
9%DOPO-POSS/FRPET	399.53	436.97	17.24	23.56

In a N$_2$ atmosphere, the thermal degradation process of PET, FRPET, and DOPO-POSS/FRPET composites was completed in one step. It can be seen from Table 3 that the initial thermal decomposition temperature ($T_{5\%}$) of PET and the carbon residue (C_w) at 700 °C are 401 °C and 16.97%, respectively. Compared with PET, the $T_{5\%}$ of FRPET decreases, indicating that CEPPA promotes the degradation of PET, while as the temperature increases, phosphorus-containing flame retardants exert a flame retarding effect. After dehydration, a carbon layer is formed on the surface of PET.[22,23] It is manifested as the decrease of maximum thermal weight loss rate (R_{max}) and the increasing amount of residual carbon to 18.16%. Compared with FRPET, the thermal decomposition temperature $T_{5\%}$ of the DOPO-POSS/FRPET composite has no obvious change, which shows that the addition of DOPO-POSS does not affect the thermal stability at the beginning of heating. The residual char of DOPO-POSS/FRPET composites increases from 18 to 23%. When the addition of DOPO-POSS increases, the formation of silicon oxide covering the surface of PET increases and the heat transfer is further suppressed. In addition, because the phosphorus-containing fragments are decomposed by heat to generate phosphoric acid, which plays a role in delaying the degradation of the polyester, R_{max} drops from 19.2 to 17.2%. It can be seen from Table 3 that under the combined effect of DOPO-POSS and CEPPA, the residual char of PET increases significantly. The carbon layer can prevent the thermal decomposition of PET, thereby increasing the thermal stability of the composites (Figure 4).[24,25]

3.4. LOI Test. The LOI provides an important data support for evaluating the combustion behavior of materials. As we all know, the LOI of PET is only 22%. It can be seen in Table 4 that the LOI of FRPET increased to 26% after adding the

Table 4. LOI and UL-94 Data of PET, FRPET, and DOPO-POSS/FRPET Composites

samples	LOI (%)	UL-94		
		t_1	$t_2 + t_3$	grade
PET	22	31.60	19.80	NR
FRPET	26	16.20	4.60	V-2
3%DOPO-POSS/FRPET	26	5.35	4.55	V-2
5%DOPO-POSS/FRPET	29	5.60	4.15	V-2
7%DOPO-POSS/FRPET	30	4.70	1.85	V-2
9%DOPO-POSS/FRPET	33	2.75	2.20	V-0

phosphorus flame retardant. It can be explained by the generation of phosphorous oxygen radicals, which captured the H$^{\bullet}$ and OH$^{\bullet}$ radicals during the combustion process, thereby inhibiting further combustion. Compared with FRPET, after adding the flame-retardant DOPO-POSS, the LOI reached 33% when the addition amount was 9 wt %. In DOPO-POSS/FRPET composites, the synergistic flame retarding effect of Si and P elements was further manifested. CEPPA played the roles of free radical quenching and dehydration into char. On the one hand, the Si−O chain link in DOPO-POSS can promote PET carbon formation.[26] On the other hand, because the POSS cage structure in DOPO-POSS decomposes and produces smaller molecules of the silane structure during the combustion process, it can enhance the carbon fixation effect of the carbon layer.

3.5. UL-94 Test. The results of the UL-94 test are shown in Table 4 as well. It can be seen that the burning time of FRPET was shortened by about 40% compared with that of pure PET, but dripping can still ignite the absorbent cotton, and the flame retardant grade can only reach V-2.

When the flame-retardant DOPO-POSS is added to the FRPET matrix, the flame burning times t_1 and t_2 both showed a significant decreasing trend, and $\sum(t_1 + t_2)$ is less than 10 s. With increasing flame retardant, the first flame burning time greatly shortened further, indicating that the addition of DOPO-POSS can shorten the flame burning time of FRPET. When the amount of DOPO-POSS was 9 wt %, the flame burning time reached the shortest value, and the phenomenon of self-extinguishing appears in the air, and the grade also reached the V-0 level. After adding DOPO-POSS, the phosphorous in FRPET interacted with the polyester during
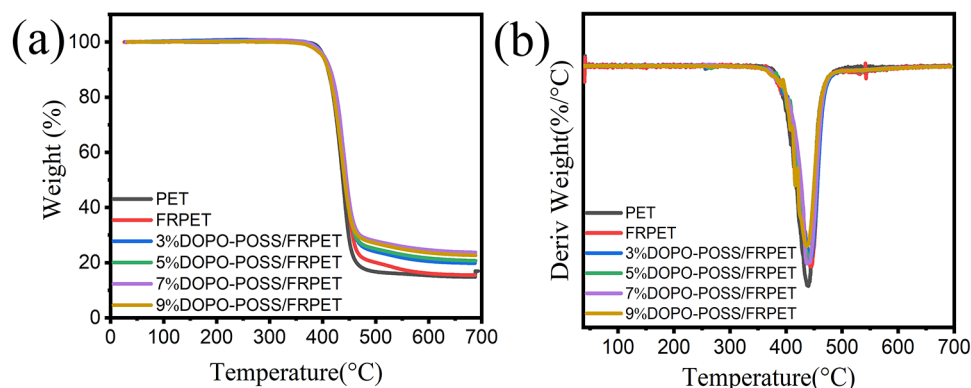

Figure 4. Thermogravimetric curves of flame-retardant PET composites. (a) TG and (b) DTG.
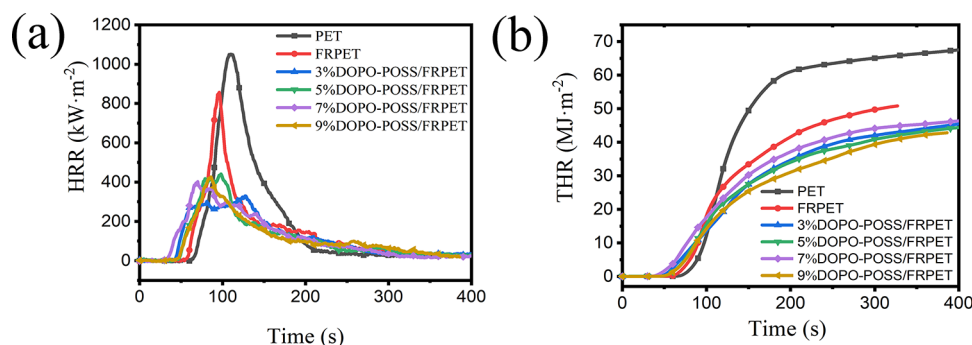
Figure 5. Cone calorimetry curves of flame-retardant FRPET composites. (a) HRR and (b) THR.

the combustion process, and the phosphoric acid and metaphosphoric acid produced by CEPPA promoted the dehydration of polyester into charcoal and covered the surface of PET, which can prevent the generated flammable small molecules from running away. Moreover, the small silane particles produced by the decomposition of DOPO-POSS covered the surface of the polyester, which can enhance the thermal stability of the carbon layer and isolate the combustible gas and air. Under the synergistic effect of phosphorus and silicon, the flame burning time of DOPO-POSS/FRPET composites shortened, and the flame retarding effect significantly improved.[27]

3.6. Cone Calorimetery Analysis. The cone calorimetry test (CONE) can effectively evaluate the combustion behavior of the polyester under air conditions. The heat release rate (HRR) is considered to be the most important variable in characterizing the flammability of materials and their consequent fire hazard.[28] The changes of HRR and THR of PET, FRPET, and DOPO-POSS/FRPET composites along with the flame time are shown in Figure 5a,b. Table 5 shows

Table 5. Cone Calorimetery Data for the PET Composites

samples	TTI (s)	p-HRR (kW·m^{-2})	m-HRR (kW·m^{-2})	THR (MJ·m^{-2})	FRI
PET	51.00	1493.64	239.13	76.03	1.00
FRPET	54.00	1026.03	182.20	63.89	34.85
3% DOPO-POSS/FRPET	39.00	348.38	107.54	48.03	46.36
5% DOPO-POSS/FRPET	43.00	441.78	104.38	46.57	47.81
7% DOPO-POSS/FRPET	39.00	402.61	118.80	47.06	47.32
9% DOPO-POSS/FRPET	44.00	420.34	112.46	42.84	51.98

the relevant data of the CONE test of the composites. It can be seen from Figure 5a,b that the HRR and THR of FRPET and DOPO-POSS/FRPET composites have significantly decreased. Compared with PET, the time to ignition (TTI) of FRPET is prolonged by 3 s, indicating that the introduction of phosphorus-containing flame retardants makes it more difficult to ignite and improves the fire resistance of PET. Phosphorus-containing fragments can capture combustible gas free radicals in the gas phase and inhibit the generation of combustible gas, thereby prolonging the ignition time of FRPET. It can be seen from Figure 5a that the peak of the HRR of PET is high and sharp, which indicates that the heat is released more and faster during the combustion process, while the width of the exothermic peak of FRPET is smaller than that of PET and

the HRR is lower. It also can be seen from Table 5 that compared with PET, the p-HRR and THR of FRPET are decreased by 31.3 and 43.4%, respectively. During the combustion process, the phosphorus-containing flame retardant promotes the formation of residue char of PET and covers the surface of the material and then insulates heat transfer and hinders the release of combustible gas.[29]

As shown in Figure 5, with the addition of DOPO-POSS, TTI decreased to 40 from 54 s of PET. Compared with FRPET, p-HRR decreased by 66.0% and THR decreased by 32.4%. After adding DOPO-POSS, the siloxy chain segment of POSS promoted the formation of the carbon layer, and the decomposition of DOPO generated metaphosphoric acid, which can also enhance the carbon layer. The continuous dense carbon layer hindered the transfer of heat insulation and delayed the heat release process of the composite during combustion.[30]

The flame retardancy index (FRI, defined by $[\text{THR} \times (\text{pHRR}/\text{TTI})]_{\text{Neat polymer}}/[\text{THR} \times (\text{pHRR}/\text{TTI})]_{\text{Composite}}$) is used to calculate for the thermoplastic composites "Poor", "Good", and "Excellent" flame retardancy performances.[31] FRI < 1 is taken as the lowest level of flame retardancy symbolized as "Poor" performance. FRI values up to 10^1 ($1 < \text{FRI} < 10$) are nominated as "Good", and the FRI values between 10^1 and below 10^2 ($10 < \text{FRI} < 100$) are labeled "Excellent". As shown in Table 5, the FRI value of PET is 1 and it has no flame retardancy, and the FRPET value is 34.85, indicating that the flame retardancy performance is significantly improved. With the addition of DOPO-POSS, the FRI value also gradually increases. When 9 wt % DOPO-POSS is used, the FRI value reaches the highest at 51.98, during the degradation of DOPO-POSS, forms compact char, which protects the polymer from fire hazards, and the FRI value reaches excellent.

3.7. Flame Retardancy Mechanism. *3.7.1. Char Residue Analysis.* The morphologies of the residual carbon at different magnifications of FRPET and 9% DOPO-POSS/FRPET composites are shown in Figure 6. It can be observed that the carbon residue of the DOPO-POSS/FRPET composites has a macroscopic appearance that the surface of the carbon layer is dense and continuous, and the height increases. We can also see that the surface of the carbon layer of the DOPO-POSS/FRPET composite is more flat, with smaller pore size and dense distribution.[32] It can be explained that the phosphorus-containing segments and the silicon−oxygen segments play a role in promoting carbon formation on the surface of PET, while the DOPO-POSS also can migrate to the PET surface after being heated and then form a more stable Si−O−C covering layer. As a result, the DOPO-POSS/FRPET composite forms a more stable and dense carbon layer
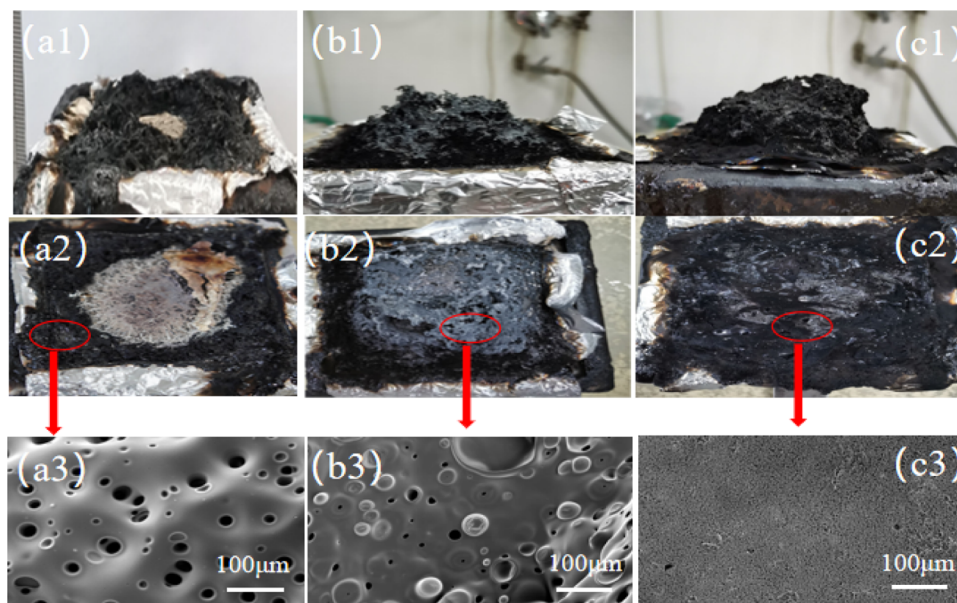
Figure 6. Digital photos and SEM images of the residual char of PET composites after the cone test: (a1, a2, a3) pure PET, (b1, b2, b3) FRPET, and (c1, c2, c3) 9%DOPO-POSS/FRPET.
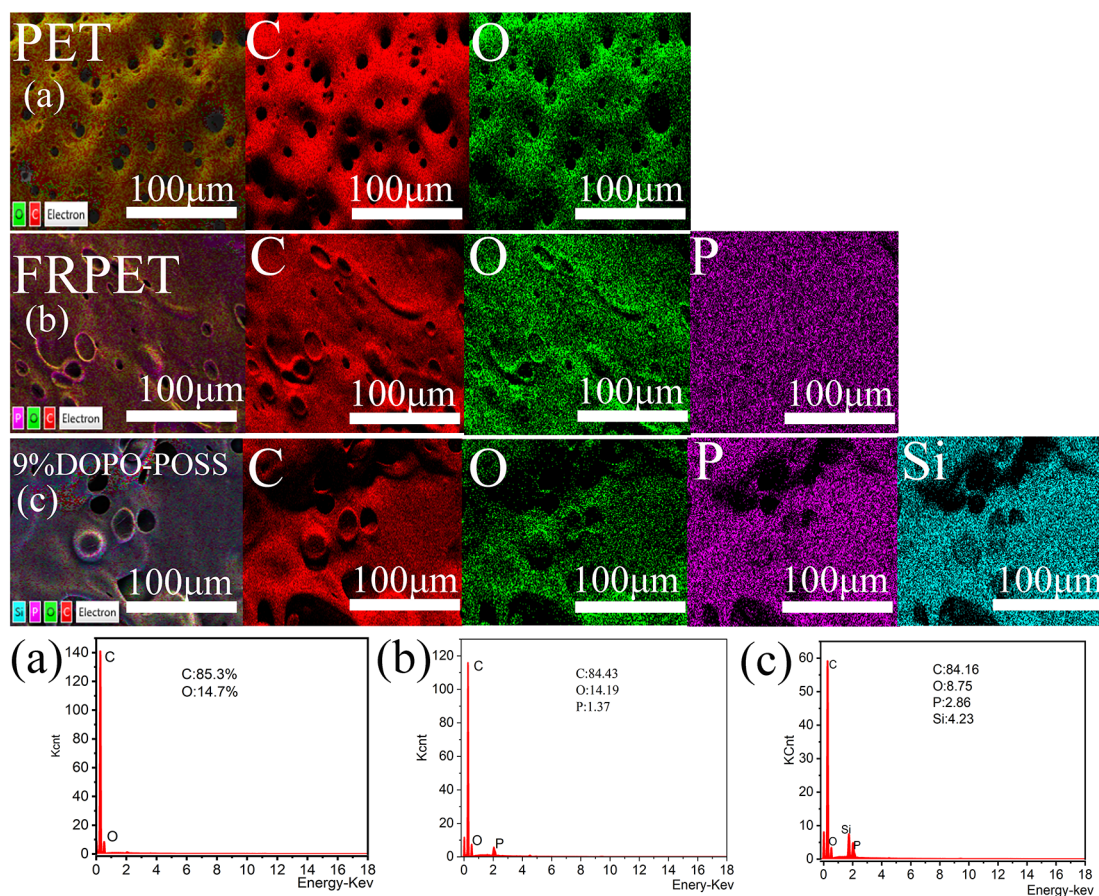

Figure 7. EDS elemental mapping of PET(a), FRPET(b), and 9%DOPO-POSS/FRPET(c).

structure, and the flame retarding performance has been significantly improved.[33]

The chemical composition and morphology of the composites were further studied by SEM combined with EDS, and the results are shown in Figure 7. The FRPET sample element concentrations as determined by SEM−EDS were 84.43% carbon, 14.19% oxygen, and 1.37% phosphorus on the exposed residual carbon surface after combustion. Compared with the pure PET with 85.3% carbon and 14.7% oxygen, for FRPET, the primary fire retardancy action is likely

to occur in the condensed phase. The corresponding 9% DOPO-POSS/FRPET residue consisted of 84.16% carbon, 8.75% oxygen, 2.86% phosphorus, and 4.23% silicon.[34] The content of phosphorus in DOPO-POSS/FRPET was significantly higher than that in FRPET. In addition, as for the residual char of 9%DOPO-POSS/FRPET, the silicon element was detected in it. Combined with the morphology of residual carbon in Figure 6 and the SEM image, during the combustion process, the P/Si element composite promotes char formation on the PET surface, increases the compactness of the carbon layer, and further improves the flame retardancy of the composite.[35,36]

To further analyze the structure of the residue after combustion, the FTIR spectra of the residue after the cone test are shown in Figure 8. As can be seen, 1748, 1621, 1100,
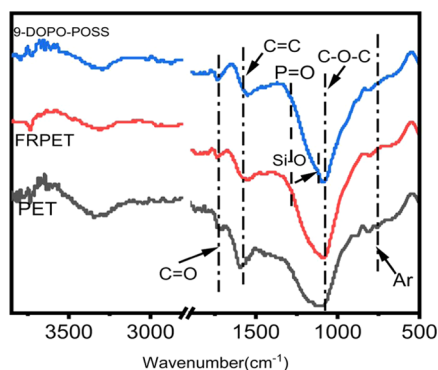

Figure 8. FTIR spectra of the char residue for PET, FRPET, and 9% DOPO-POSS/FRPET.

and 750 cm⁻¹ correspond to the C=O, C=C, C−O−C, and benzene ring stretching vibration peaks in the residual char of PET, indicating that the residual char contains a lot of benzene rings and ester structures. Compared with pure PET, the residual char of FRPET and 9%DOPO-POSS/FRPET shows a new stretching vibration peak appearing at 1280 cm⁻¹ corresponding to P=O, indicating the presence of phosphorus, which plays an important role in delaying combustion. As for 9%DOPO-POSS/FRPET, the stretching vibration peak of the Si−O bond appears near 1080 cm⁻¹, which also proves the existence of Si after combustion. The protective layer formed in the residue of 9%DOPO-POSS/FRPET enhances the barrier effect, and then, the DOPO-POSS shows a more effective effect of condensed-phase flame retardancy.

A Raman spectrometer was used to further characterize the degree of graphitization and regularity of the carbon layer after combustion, and the Raman spectra of PET, FRPET, and 9% DOPO-POSS/FRPET are shown in Figure 9. As we can see, there are two obvious peaks named D band (1340 cm⁻¹) and G band (1596 cm⁻¹). They represent the disordered or amorphous carbon and the stretching vibration peak of the ordered carbon C=C, respectively. The area ratios of the D band and G band (A_D/A_G) calculated by peak splitting indicate the degree of graphitization of the carbon layer. We use Peakfit software to process and then select the A_D/A_G value obtained after fitting the curve with Gauss Lor amp. A lower A_D/A_G value means a higher graphitization degree of char. As we can see in Figure 9, the A_D/A_G of the pure PET char residue is 2.18, while the A_D/A_G of the FRPET char residue decreases to 2.04, indicating that CEPPA can promote carbon formation in the condensed phase and the degree of graphitization of char is higher than that of PET. Furthermore, the A_D/A_G of 9% DOPO-POSS/FRPET is only 1.86, which is lower than that of pure PET and FRPET. The addition of DOPO-POSS further increases the degree of graphitization of the carbon layer, which further proves the blocking effect of the Si-containing char layers in the condensed phase.[37,38]

3.7.2. Gas Volatile Analysis. To understand the flame retardancy mechanism of the composites deeply, the TG-FTIR technology is used to analyze the gas-phase products of PET, FRPET, and 9%DOPO-POSS/FRPET during the process of thermal degradation. The 3D TG-FTIR spectra of the gas phase for the decomposition and the infrared spectra at 430 °C in a nitrogen atmosphere of PET and its composites are shown in Figure 10. As seen from the 3D graph, there are almost no other peaks except for the release of CO_2 below 400 °C. As the temperature continues to increase to T_{max} (430 °C), the FTIR spectra of PET, FRPET, and 9%DOPO-POSS/FRPET exhibit obvious peaks of stretching vibrations, such as 2753, 2350, 1765, and 743 cm⁻¹, which correspond to the structures of alkanes, CO_2, C=O, and benzene rings, respectively. It is worth noting that FRPET and 9% DOPO-POSS/FRPET have P=O bonds at 1258 cm⁻¹ and Si−O bonds are detected at 1108 cm⁻¹, indicating that the degradation of DOPO-POSS and CEPPA promotes the formation of a protective char layer, which could prevent the combustible gases from transferring to the surface of the materials and feeding the flame.[39,40] Meanwhile, the release of nonflammable gases can dilute the combustible gas.[41]

3.7.3. Py−GC−MS. To further understand the thermal degradation process of PET and clarify the flame retardancy
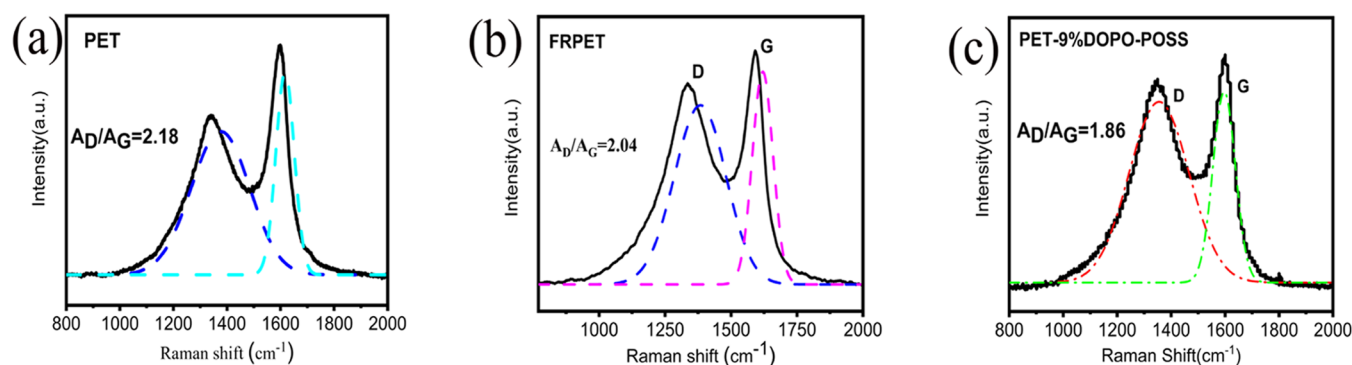

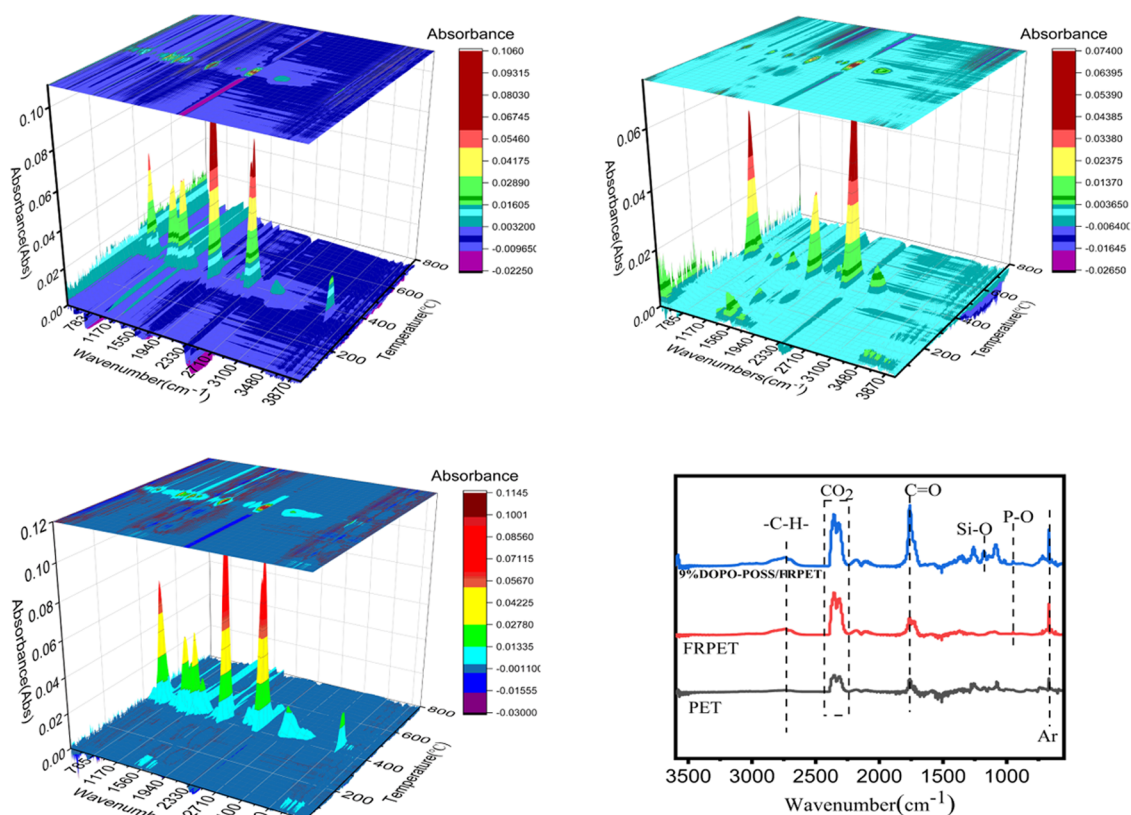**Figure 9.** Raman spectra of PET, FRPET, and 9%DOPO-POSS/FRPET.

Figure 10. 3D TG-FTIR spectra and FTIR spectra at 430 °C by TG-FTIR for pure PET, FRPET, and 9%DOPO-POSS/FRPET.

Table 6. Tensile Properties of PET and Its Composites

samples	tensile strength (MPa)	elastic modulus (MPa)	elongation (%)
PET	50.45	685.1	313
FRPET	49.03	682.3	330
3% DOPO-POSS/FRPET	48.92	642.2	323
5% DOPO-POSS/FRPET	47.98	703.6	278
7% DOPO-POSS/FRPET	48.43	703.7	80
9%DOPO-POSS/FRPET	43.82	700.1	60

Table 7. Compounds Identified in the Pyrograms of PET, FRPET, and DOPO-POSS/FRPET

		content (%)	
no.	name	PET	FRPET
1	vinyl benzoate	1.18	1.11
2	benzoic acid	47.73	6.33
3	nenzoic acid, 4-methyl-	0.80	1.03
4	4-ethylbenzoic acid	1.66	2.01
5	4-vinylbenzoic acid	1.59	
6	P-formyl radical benzoic acid	0.43	6.06
7	4-formyl radical benzoic acid ethyl radical ester	1.67	1.16
8	terephthalic acid, 2-chlorophen	0.32	0.81
9	1,4-benzenedicarboxylic acid	28.16	62.03
10	biphenyl-4-carboxylic acid	2.01	
11	benzoic anhydride	3.33	
12	segments of the PET	1.58	3.33
13	diisopropyl phenylphosphonite		1.55
14	phenylphosphonous acid		2.66
15	benzophenone-2,4′-dicarboxylic acid		1.12

no.	name	content (%) 9%DOPO-POSS/FRPET
1	2-hydroxyethyl hydrogen vinylphosphonate	25.31
2	benzoic acid	15.75
3	benzoic acid, 2-(1-oxopropyl)-	8.73
4	9,10-dihydro-9-oxa-10-phosphaphenanthrene-10-oxide	16.43
5	phenol, 4,4′-(1-methylethylidene)bis-	16.82
6	segments of the PET	8.14
7	silane, diethylhexadecyloxy(3-methylbutoxy)-	2.53

degradation mechanism during the combustion process, the Py−GC−MS test was used to explore the degradation products in the gas phase of PET, FRPET, and 9%DOPO-POSS/FRPET. The detailed data are listed in Table 7, and the thermal decomposition process is shown in Figures 11 and 12. The main pyrolysis products of pure PET are benzoic acid, 47.73%, 1,4-benzenedicarboxylic acid, 28.16%, benzoic anhydride, 3.33%, and carbon dioxide. The degradation products of FRPET are mainly 1,4-benzenedicarboxylic acid, 62.03%, P-formyl radical benzoic acid, 6.06%, benzoic acid, 6.33%, and some phosphorus-containing aromatic hydrocarbon fused ring compounds. The content of benzoic acid significantly reduced, indicating that the degradation of PET is inhibited.[42] The increase of 1,4-benzenedicarboxylic acid and the emergence of phosphorus-containing aromatic compounds showed that the PO• free radicals produced by the cracking of phosphate esters can capture other free radicals produced by decomposition, and the generated phosphate esters are dehydrated into carbon

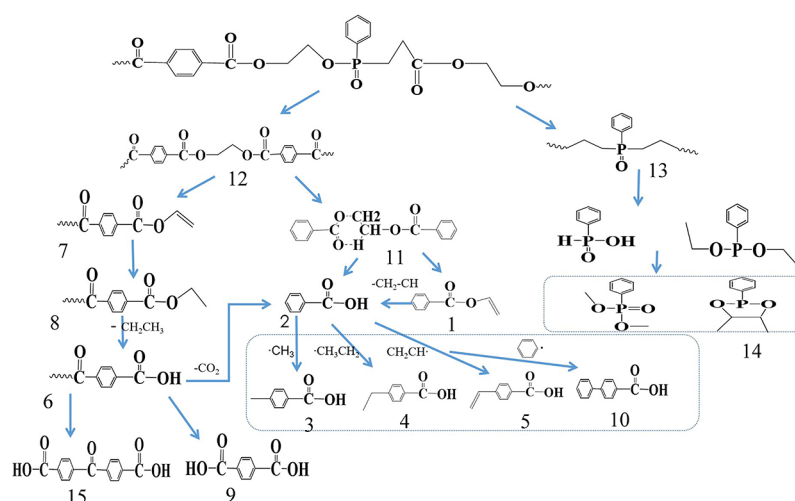**Figure 11.** Proposed pyrolysis processes for PET and FRPET.
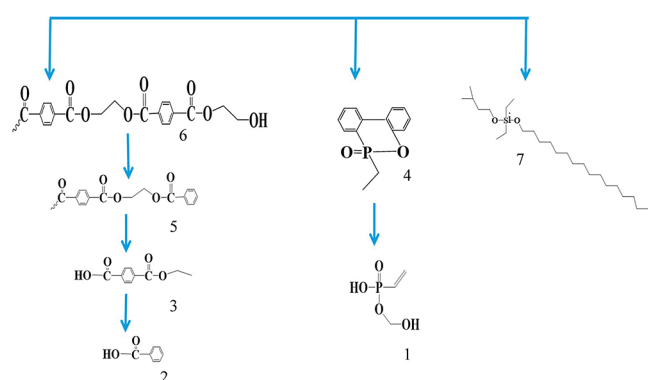
Figure 12. Proposed pyrolysis processes for 9%DOPO-POSS/FRPET.

Figure 13. Possible flame retardancy mechanism of DOPO-POSS/FRPET.

on the combustion surface, effectively blocking the heat transfer between the interior and the exterior of the matrix.

Compared with PET and FRPET, the pyrolysis products of 9%DOPO-POSS/FRPET are mainly 2-hydroxyethyl hydrogen vinylphosphonate, 25.31%, benzoic acid, 15.75%, and 9,10-dihydro-9-oxa-10-phosphaphenanthrene-10-oxide, 16.43%. Since the eight R groups of DOPO-POSS are all DOPO, in the process of degradation, phosphorus-containing substances are significantly increased and the degradation process is significantly inhibited.[43] Moreover, there are many silicon-containing compounds, which cover the surface of the dehydrated carbon layer and are firmly fixed on the surface of the carbon layer to form a more stable and dense residual carbon structure.[44]

Based on the above-mentioned analysis of the carbon morphology, carbon structure, and degradation products during combustion, the possible flame retardancy mechanism is proposed, and the mechanism diagram is shown in Figure 13. In the combustion process, the PO• free radicals released by CEPPA and DOPO can be quickly captured by the free radicals in the chain. During the process of combustion, metaphosphoric acid and other substances are generated, which promote the dehydration of the material into charcoal and effectively reduce the heat release. The cage structure of DOPO-POSS also degrades into a chain-like siloxane structure covering the surface of the carbon layer, enhancing the
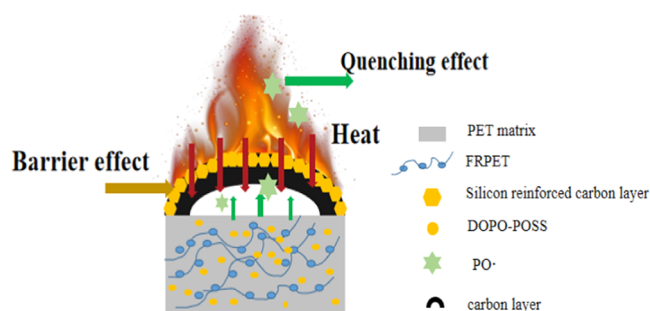
compactness and continuity of the carbon layer. Therefore, the flame retardancy mechanism of DOPO-POSS/FRPET is mainly the quenching mechanism of gas-phase free radicals and char formation in the condensed phase.

3.8. Mechanical Properties. To determine the mechanical properties of PET, FRPET, and composites with different amounts of DOPO-POSS, an INSTRON 5966 electronic material testing machine was used to test the tensile properties of the prepared standard specimens. The relevant data of pure PET and its composites are shown in Table 6.

The tensile strength of PET is 50.45 MPa, the elastic modulus is 685.1 MPa, and the elongation at break is 313%. After adding CEPPA, the tensile strength and elastic modulus of FRPET experience little effect, and the elongation at break increases slightly because CEPPA enters the main chain of PET through copolymerization and the side group of CEPPA is a large-sized benzene ring structure.[45] The results correspond to those of DSC, which show that the addition of phosphorus-containing flame retardants makes PET crystallization difficult, and then, the toughness of the polymer increases. Compared with FRPET, the addition of DOPO-POSS has little change in tensile strength at low dosages because it has better compatibility with the matrix under this condition.[46] When the amount of DOPO-POSS increases to 7 wt % or above, the cage structure of DOPO-POSS increases the spacing of FRPET molecular chains, which decreases the interaction forces between the molecules and then generates stress concentration points during the stretching process. The stress concentration points will lead to a significant decrease in

the tensile strength and elongation at break of the DOPO-POSS/FRPET composite (Table 6).[47]

4. CONCLUSIONS

DOPO-POSS/FRPET composites are prepared by melt blending, and DOPO-POSS achieves good dispersion in FRPET. It is found that DOPO-POSS reduces the crystallization performance of FRPET, and the low addition amount of DOPO-POSS has little effect on its mechanical properties. TG tests show that the addition of 9%DOPO-POSS increases the carbon residue at 700 °C by 22.9%. When the addition of DOPO-POSS reaches 9 wt %, the LOI can reach 33%, and the UL-94 test reached the V-0 level. In the cone calorimetry test, 9%DOPO-POSS/FRPET shows good flame retardancy, the FRI value reaches excellent, and the HRR and THR are reduced by 66.0 and 32.4%, respectively. We can see from the morphology of the residual carbon that the amount of residual char increases significantly and the solid-phase layer is dense and stable. Then, it is clarified that the flame retardancy mechanism of DOPO-POSS/FRPET is mainly facilitated by the PO$^\bullet$ generated by the degradation of CEPPA during the combustion process, which significantly enhances the quenching effect of gas-phase free radicals. What is more is that the degradation of phosphorus-based flame retardants promotes the dehydration of the matrix into carbon, resulting in phosphoric acid and polymetaphosphoric acid, covering the surface of the carbon layer, and the cage structure of DOPO-POSS generates silicon-containing compounds during the degradation process to cover the surface of the carbon layer and effectively block heat and mass transfer.

■ AUTHOR INFORMATION

Corresponding Authors

Guo Zheng − *School of Material Science and Engineering, Tiangong University, Tianjin 300387, China;* Email: zhengguo0703@126.com

Rui Wang − *School of Materials Design and Engineering, Beijing Institute of Fashion Technology, Beijing 100029, China;* Email: clywangrui@bift.edu.cn

Authors

Anying Zhang − *School of Material Science and Engineering, Tiangong University, Tianjin 300387, China; School of Materials Design and Engineering, Beijing Institute of Fashion Technology, Beijing 100029, China;* ⓘ orcid.org/0000-0001-5189-759X

Wenhui Wang − *School of Materials Design and Engineering, Beijing Institute of Fashion Technology, Beijing 100029, China*

Zhenfeng Dong − *School of Materials Design and Engineering, Beijing Institute of Fashion Technology, Beijing 100029, China*

Jianfei Wei − *School of Materials Design and Engineering, Beijing Institute of Fashion Technology, Beijing 100029, China;* ⓘ orcid.org/0000-0003-4834-8623

Lifei Wei − *Shanghai Different Advanced Material Company Limited, Shanghai 201502, China*

Weiwen Gu − *School of Materials Design and Engineering, Beijing Institute of Fashion Technology, Beijing 100029, China*

Complete contact information is available at:
https://pubs.acs.org/10.1021/acsomega.2c04628

Notes

The authors declare no competing financial interest.

■ REFERENCES

(1) Gooneie, A.; Simonetti, P.; Salmeia, K. A.; Gaan, S.; Hufenus, R.; Heuberger, M. P. Enhanced PET processing with organophosphorus additive: Flame retardant products with added-value for recycling. *Polym. Degrad. Stab.* **2019**, *160*, 218−228.

(2) Gooneie, A.; Simonetti, P.; Rupper, P.; Nazir, R.; Jovic, M.; Gaan, S.; Heuberger, M. P.; Hufenus, R. Stabilizing effects of novel phosphorus flame retardant on PET for high-temperature applications. *Mater. Lett.* **2020**, *276*, No. 128225.

(3) Bascucci, C.; Duretek, I.; Lehner, S.; Holzer, C.; Gaan, S.; Hufenus, R.; Gooneie, A. Investigating thermomechanical recycling of poly(ethylene terephthalate) containing phosphorus flame retardants. *Polym. Degrad. Stab.* **2022**, *195*, No. 109783.

(4) Chu, F.; Qiu, S.; Zhou, Y.; Zhou, X.; Cai, W.; Zhu, Y.; He, L.; Song, L.; Hu, W. Novel glycerol-based polymerized flame retardants with combined phosphorus structures for preparation of high performance unsaturated polyester resin composites. *Composites, Part B* **2022**, *233*, No. 109647.

(5) Li, Q.; Zhang, S.; Mahmood, K.; Jin, Y.; Huang, C.; Huang, Z.; Zhang, S.; Ming, W. Fabrication of multifunctional PET fabrics with flame retardant, antibacterial and superhydrophobic properties. *Prog. Org. Coat.* **2021**, *157*, No. 106296.

(6) Zhang, C.; Zhang, C.; Hu, J.; Jiang, Z.; Zhu, P. Flame-retardant and anti-dripping coating for PET fabric with hydroxyl-containing cyclic phosphoramide. *Polym. Degrad. Stab.* **2021**, *192*, No. 109699.

(7) Didane, N.; Giraud, S.; Devaux, E.; Lemort, G. A comparative study of POSS as synergists with zinc phosphinates for PET fire retardancy. *Polym. Degrad. Stab.* **2012**, *97*, 383−391.

(8) Liu, C.; Chen, T.; Yuan, C. H.; Song, C. F.; Chang, Y.; Chen, G. R.; Xu, Y. T.; Dai, L. Z. Modification of epoxy resin through the self-assembly of a surfactant-like multi-element flame retardant. *J. Mater. Chem. A* **2016**, *4*, 3462−3470.

(9) Xu, F.; Zhang, G.; Wang, P.; Dai, F. A novel ε-polylysine-derived durable phosphorus-nitrogen-based flame retardant for cotton fabrics. *Cellulose* **2021**, *28*, 3807−3822.

(10) Jia, P.; Cheng, W.; Lu, J.; Yin, Z.; Xu, Z.; Cheng, L.; Qiu, Y.; Qian, L.; Hu, Y.; Hu, W.; Wang, B. Applications of GO/OA-POSS Layer-by-Layer self-assembly nanocoating on flame retardancy and smoke suppression of flexible polyurethane foam. *Polym. Adv. Technol.* **2021**, *32*, 4516−4530.

(11) Zheng, T.; Wang, W.; Liu, Y. A novel phosphorus-nitrogen flame retardant for improving the flame retardancy of polyamide 6: Preparation, properties, and flame retardancy mechanism. *Polym. Adv. Technol.* **2021**, *32*, 2508−2516.

(12) Wang, F.; Wei, H.; Liu, C.; Sun, H.; Zhu, Z.; Liang, W.; Li, A. Monolithic nanoporous polymers bearing POSS moiety as efficient flame retardant and thermal insulation materials. *React. Funct. Polym.* **2019**, *143*, No. 104345.

(13) Hu, R.; He, K.; Zheng, X.; Zeng, B.; Chen, G.; Xu, Y.; Yuan, C.; Luo, W.; Dai, L. Preparation and properties of flame retardant epoxy resin modified by additive nitrogen-containing POSS-based molecule with eight DOPO units. *J. Polym. Res.* **2021**, *28*, No. 195.

(14) Kukla, P.; Greiner, L.; Eibl, S.; Döring, M.; Schönberger, F. Novel phosphorus-containing silazanes as flame retardants in epoxy resins. *React. Funct. Polym.* **2022**, *170*, No. 105120.

(15) Sirin, H.; Turan, D.; Ozkoc, G.; Gurdag, S. POSS reinforced PET based composite fibers: "Effect of POSS type and loading level". *Composites, Part B* **2013**, *53*, 395−403.

(16) Qian, X.; Liu, Q.; Zhang, L.; Li, H.; Liu, J.; Yan, S. Synthesis of reactive DOPO-based flame retardant and its application in rigid polyisocyanurate-polyurethane foam. *Polym. Degrad. Stab.* **2022**, *197*, No. 109852.

(17) Oh, J.; Kim, S. S.; Lee, J.; Kang, C. Supercritical fluid flame-retardant processing of polyethylene terephthalate (PET) fiber treated with 9, 10-dihydro-9-oxa-10-phosphaphenanthrene-10-oxide (DOPO): Changes in physical properties and flame-retardant performance. *J. CO2 Util.* **2021**, *54*, No. 101761.

(18) He, M.; Zhang, D.; Zhao, W.; Qin, S.; Yu, J. Flame retardant and thermal decomposition mechanism of poly(butylene tereph-thalate)/DOPO-HQ composites. *Polym. Compos.* **2019**, *40*, 974−985.

(19) Miniewicz, A.; Tomkowicz, M.; Karpinski, P.; Sznitko, L.; Mossety-Leszczak, B.; Dutkiewicz, M. Light sensitive polymer obtained by dispersion of azo-functionalized POSS nanoparticles. *Chem. Phys.* **2015**, *456*, 65−72.

(20) Ozimek, J.; Sternik, D.; Radzik, P.; Hebda, E.; Pielichowski, K. Thermal degradation of POSS-containing nanohybrid linear polyur-ethanes based on 1,6-hexamethylene diisocyanate. *Thermochim. Acta* **2021**, *697*, No. 178851.

(21) Muhammad, S.; Niazi, J. H.; Shawuti, S.; Qureshi, A. Functional POSS based polyimide nanocomposite for enhanced structural, thermal, antifouling and antibacterial properties. *Mater. Today Commun.* **2022**, *31*, No. 103287.

(22) Li, S.; Zhao, X.; Zhang, Y.; Yang, X.; Yu, R.; Zhang, Y.; Deng, K.; Huang, W. A facile approach to prepare cage-ladder-structure phosphorus-containing amino-functionalized POSS for enhancing flame retardancy of epoxy resins. *J. Appl. Polym. Sci.* **2020**, *138*, No. 49870.

(23) Zhang, W.; Li, X.; Yang, R. Pyrolysis and fire behaviour of epoxy resin composites based on a phosphorus-containing polyhedral oligomeric silsesquioxane (DOPO-POSS). *Polym. Degrad. Stab.* **2011**, *96*, 1821−1832.

(24) Song, L.; He, Q.; Hu, Y.; Chen, H.; Liu, L. Study on thermal degradation and combustion behaviors of PC/POSS hybrids. *Polym. Degrad. Stab.* **2008**, *93*, 627−639.

(25) Wang, H.; Li, X.; Su, F.; Xie, J.; Xin, Y.; Zhang, W.; Liu, C.; Yao, D.; Zheng, Y. Core-Shell ZIF67@ZIF8 Modified with Phytic Acid as an Effective Flame Retardant for Improving the Fire Safety of Epoxy Resins. *ACS Omega* **2022**, *7*, 21664−21674.

(26) Jin, W.-J.; Cheng, X.-W.; He, W.-L.; Gu, L.; Li, S.; Gou, Y.-W.; Guan, J.-P.; Chen, G. Flame retardant and anti-dripping modification of polyamide 6 fabric by guanidine sulfamate with enhanced durability. *Thermochim. Acta* **2021**, *706*, No. 179073.

(27) Wang, C.; Wu, L.; Dai, Y.; Zhu, Y.; Wang, B.; Zhong, Y.; Zhang, L.; Sui, X.; Xu, H.; Mao, Z. Application of self-templated PHMA sub-microtubes in enhancing flame-retardance and anti-dripping of PET. *Polym. Degrad. Stab.* **2018**, *154*, 239−247.

(28) Quan, Y.; Zhang, Z.; Tanchak, R. N.; Wang, Q. A review on cone calorimeter for assessment of flame-retarded polymer composites. *J. Therm. Anal. Calorim.* **2022**, *147*, 10209−10234.

(29) Liu, J.; Kong, D.; Dong, C.; Zhang, Z.; Wang, S.; Sun, H.; Lu, Z. Preparation of a novel P/Si polymer and its synergistic flame retardant application on cotton fabric. *Cellulose* **2021**, *28*, 8735−8749.

(30) Barletta, M.; Aversa, C.; Ayyoob, M.; Gisario, A.; Hamad, K.; Mehrpouya, M.; Vahabi, H. Poly(butylene succinate) (PBS): Materials, processing, and industrial applications. *Prog. Polym. Sci.* **2022**, *132*, No. 101579.

(31) Vahabi, H.; Kandola, B. K.; Saeb, M. R. Flame Retardancy Index for Thermoplastic Composites. *Polymers* **2019**, *11*, No. 407.

(32) Vannier, A.; Duquesne, S.; Bourbigot, S.; Castrovinci, A.; Camino, G.; Delobel, R. The use of POSS as synergist in intumescent recycled poly(ethylene terephthalate). *Polym. Degrad. Stab.* **2008**, *93*, 818−826.

(33) Chen, X.; Wang, B.; Hao, Z.; Tan, G.; Selim, M. S.; Yu, J.; Huang, Y. Synergistic Effect of Multifunctional Layered Double Hydroxide-Based Hybrids and Modified Phosphagen with an Active Amino Group for Enhancing the Smoke Suppression and Flame Retardancy of Epoxy. *ACS Omega* **2022**, *7*, 21714−21726.

(34) Zhang, C.; Wang, J.; Song, S. Preparation of a novel type of flame retardant diatomite and its application in silicone rubber composites. *Adv. Powder Technol.* **2019**, *30*, 1567−1575.

(35) Yuan, G.; Yang, B.; Chen, Y.; Jia, Y. Synthesis of a novel multi-structure synergistic POSS-GO-DOPO ternary graft flame retardant and its application in polypropylene. *Composites, Part A* **2019**, *117*, 345−356.

(36) Yu, S.-j.; Lu, S.-y.; Tan, D.-f.; Zhu, Y.-F. Nitrogen and phosphorus co-doped carbon dots for developing highly flame retardant poly (vinyl alcohol) composite films. *Eur. Polym. J.* **2022**, *164*, No. 110970.

(37) Zhang, P.; Ma, D.; Cheng, J.; Zhang, X.; Chen, X. Effects of hexaphenoxycyclotriphosphazene and glass fiber on flame-retardant and mechanical properties of the rigid polyurethane foam. *Polym. Compos.* **2020**, *41*, 3521−3527.

(38) Zhang, W.; Li, X.; Yang, R. Flame retardancy mechanisms of phosphorus-containing polyhedral oligomeric silsesquioxane (DOPO-POSS) in polycarbonate/acrylonitrile-butadiene-styrene blends. *Polym. Adv. Technol.* **2012**, *23*, 588−595.

(39) Jia, L.; Zhang, W.-C.; Tong, B.; Yang, R.-J. Crystallization, Mechanical and Flame-retardant Properties of Poly(lactic acid) Composites with DOPO and DOPO-POSS. *Chin. J. Polym. Sci.* **2018**, *36*, 871−879.

(40) Shao, Z.-B.; Cui, J.; Li, X.-L.; Díaz Palencia, J. L.; Wang, D.-Y. Chemically inorganic modified ammonium polyphosphate as eco-friendly flame retardant and its high fire safety for epoxy resin. *Compos. Commun.* **2021**, *28*, No. 100959.

(41) Zhan, J.; Wang, J.; Lin, J.; Zhao, G.; Ji, S.; Li, X.; Li, J.; Wang, G.; Chen, L.; Guan, Y.; Naceur, H. Flame-retardant, thermal and mechanical properties of PLA/ramie fiber composites. *Polym. Compos.* **2022**, *43*, 4244−4254.

(42) Fang, Y.; Liu, X.; Wu, Y. High efficient flame retardant finishing of PET fabric using eco-friendly DOPO. *J. Text. Inst.* **2022**, *113*, 1248−1255.

(43) Forchetti Casarino, A.; Casis, N.; Estenoz, D. A.; Spontón, M. E. Synthesis and characterization of polybenzoxazine/silica-based hybrid nanostructures for flame retardancy applications. *Polym. Eng. Sci.* **2022**, *62*, 1386−1398.

(44) Dai, X.; Li, P.; Sui, Y.; Zhang, C. Thermal and flame-retardant properties of intrinsic flame-retardant epoxy resin containing biphenyl structures and phosphorus. *Eur. Polym. J.* **2021**, *147*, No. 110319.

(45) Zhang, W.; Li, X.; Guo, X.; Yang, R. Mechanical and thermal properties and flame retardancy of phosphorus-containing polyhedral oligomeric silsesquioxane (DOPO-POSS)/polycarbonate composites. *Polym. Degrad. Stab.* **2010**, *95*, 2541−2546.

(46) Vahabi, H.; Laoutid, F.; Formela, K.; Saeb, M. R.; Dubois, P. Flame-Retardant Polymer Materials Developed by Reactive Extrusion: Present Status and Future Perspectives. *Polym. Rev.* **2022**, *62*, 919−949.

(47) Li, J.; Wu, W.; Hu, H.; Rui, Z.; Zhao, T.; Zhang, X. The synergism effect of montmorillonite on the intumescent flame retardant thermoplastic polyurethane composites prepared by selective laser sintering. *Polym. Compos.* **2022**, *43*, 5863−5876.